Resource Allocation in Protected and Shared Bands: Uniqueness and Efficiency of Nash Equilibria*

Rami Mochaourab and Eduard Jorswieck
Communications Theory, Communications Laboratory
Dresden University of Technology, Dresden, Germany
{Mochaourab, Jorswieck}@ifn.et.tu-dresden.de

ABSTRACT

Motivated by the question, is non-cooperative spectrum sharing desirable or not, we consider a scenario utilizing protected and shared bands. In a static non-cooperative setting consisting of two communication system pairs, we study the existence, uniqueness and efficiency of a fixed point of the iterative water-filling algorithm which corresponds to the Nash equilibrium. There exist several sufficient conditions for the convergence of the algorithm in the literature mostly based on the contraction mapping theorem. We derive necessary and sufficient conditions for convergence by relating the game to supermodular games. There, the best response dynamics is globally convergent when a unique Nash equilibrium exists. In order to understand the loss in efficiency due to non-cooperation, we study the Price of Anarchy of the system. We show that the performance of the non-cooperative system cannot fall below two third of that of the cooperative system in the high signal to noise ratio regime. Theoretical results are illustrated by numerical simulations for a simplified system scenario.

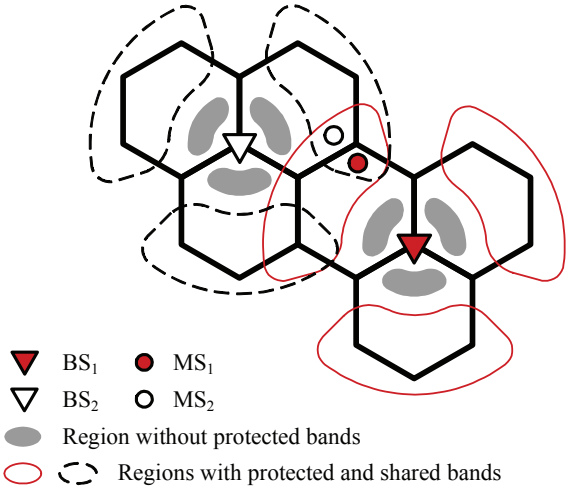

Figure 1: Illustration of a Mobile WiMAX scenario with two base stations and two mobile stations.

1. INTRODUCTION

In order to maximize the spectral efficiency of the wireless communication system, Mobile WiMAX [1] supports frequency reuse of one, i.e. the same frequency channels are used in every cell. This in turn, brings about the problem of co-channel interference at cell edges where in such regions the quality of service (QoS) is downgraded. Mobile WiMAX, which has the channel bandwidth divided into several subchannels, utilizes fractional frequency reuse (FFR) [2] in order to deal with the cell edge interference problem. The idea of applying FFR is to partially enable spectrum sharing and partially assure independent use of the channel.

In a non-cooperative scenario, spectrum sharing might lead to suboptimal operating points or equilibria [3]. Considering competition between wireless networks, the non-cooperative operating strategy of the systems is studied in [4]. Operation regimes are examined and determined by the authors where the strategies of the networks correspond to the link scheduling procedure. The case of distributed resource allocation and the conflicts in non-cooperative spectrum sharing is best analyzed in a non-cooperative game theoretic approach. An overview of power control using game theory is presented in [5, 6]. Moreover, analysis of non-cooperative and cooperative settings using game theory are performed in [7].

Similar work to ours is presented in [8, 9]. In [8], the authors characterize the uniqueness conditions for a Nash equilibrium (NE) in the game with two communication system pairs sharing two parallel bands non-cooperatively. In [9], two system pairs are considered that operate on two parallel channels, an interference channel and an interference relay channel. Two relaying strategies are investigated for which the uniqueness conditions of the NE are derived. In both works the global convergence properties of the best response dynamics are not investigated. Note that the uniqueness conditions of the NE does not directly imply the global convergence of an iterative method to this fixed point. The scenario of protected and shared bands is considered in [10], where the manipulability of the NE is studied for two cells each consisting of a base station and multiple mobile stations. In order to enforce truthful operation, an incentive

*This work is supported in part by the Deutsche Forschungsgemeinschaft (DFG) under grant Jo 801/4-1.

Gamecomm 2009, October 23, 2009 - Pisa, Italy.

Digital Object Identifier: 10.4108/ICST.VALUETOOLS2009.7793
http://dx.doi.org/10.4108/ICST.VALUETOOLS2009.7793

compatible mechanism is adopted for a game with incomplete information in each cell. This in turn allows a game with complete information between the two cells.

The optimal power allocation strategy for one user for fixed interference power corresponds to the water-filling solution [11]. For each user, his strategy depends on the power allocations of the other users. Therefore, in non-cooperative scenarios the users need to update their power allocations iteratively. This iterative adjustment of power levels is called the iterative water-filling algorithm (IWF). On convergence of the algorithm, the operation point corresponds to the NE. In a wireless scenario, there may exist several NEs, which in turn compromises the convergence of the algorithm. Several work has been done to study the uniqueness of the NE and convergence of the IWF as in [12–15]. In [16], the convergence of a distributed power control algorithm in fading interference systems is proven.

An illustration of a Mobile WiMAX scenario is given in Fig. 1. There exist two base stations, BS_1 and BS_2, and three distinctive sets of sub-channels, f_1, f_2, and f_3. If BS_1 operates on f_1 and f_2 and BS_2 on f_1 and f_3, the system pair $BS_1 \rightarrow MS_1$ can use f_2 without experiencing interference from $BS_2 \rightarrow MS_2$. We call f_2 *protected* for the first pair, and similarly is f_3 protected for the second. The remaining sub-channel set f_1 can be accessed by both system pairs and hence is denoted as *shared*.

The contributions of this work are twofold:

- We characterize the uniqueness conditions of the NE in our non-cooperative spectrum sharing game. We show that the game belongs to the class of supermodular games. Therefore, uniqueness of NE implies global convergence of the IWF.
- We analyze whether the shared band is used for spectrum sharing. For these circumstances we study the efficiency of the outcome of the non-cooperative game.

The paper is organized as follows: In section 2, we describe the system model along with the channel and game model. In section 3, we begin by defining supermodular games. Utilizing the properties of such games, we proceed to characterize the conditions for the uniqueness of the NE which directly lead to the characterization of the convergence conditions for the IWF algorithm. Afterwards, the efficiency of the system is studied. Conclusions are drawn over the acquired results in section 4.

2. PRELIMINARIES

2.1 System Model

As in Fig. 1, we consider two communication system pairs each consisting of a base station BS_i and a mobile station MS_i, $i = 1, 2$. Each base station is assumed to be the transmitter to its corresponding mobile station of the same subscript. On operating in the same bands, both systems interfere on one another. This model can be easily extended to multiple system pairs. We focus on two pairs for convenience.

By utilizing OFDM, the spectrum is divided into several parallel frequency flat channels. In this way, each system pair can operate on one of these bands privately without witnessing interference from the other pair. We assume for our two-system pair scenario that there exists three bands,

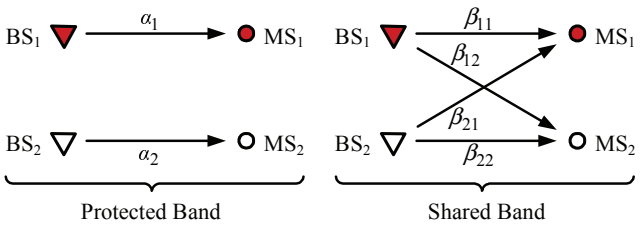

Figure 2: Illustration of the protected and shared bands.

and these are assigned in the following way: One band is allocated for each system pair to use privately and denoted as protected, and one band is used by both system pairs constituting a Gaussian interference channel (IFC) denoted as shared.

2.2 Channel Model

The instantaneous channel gains in the protected bands are denoted as h_i^p, and in the shared band as h_{ij}^s, $i, j = 1, 2$. The fading channel coefficients, which are the squared amplitude of the channel gains, are given as $\alpha_i = |h_i^p|^2$ and $\beta_{ij} = |h_{ij}^s|^2$ (see Fig. 2). In addition, the noise power is represented by σ^2. Each system has a sum power constraint of P, $P > 0$, to allocate in the shared plus protected bands. The signal to noise ratio (SNR) is given by $\rho = \frac{P}{\sigma^2}$. In a non-cooperative setting, the transmitters are known to invest all power allowed, hence allocate the maximum of P between the available bands. We assume that complete instantaneous channel state information (CSI) is present at each transmitter. Based on this information, each transmitter determines how to split the power in each of its two bands in order to maximize its rate at the corresponding receiver.

2.3 Game Model

In game theoretic form [17], a game consists of a set of players, a set of strategies for each player, and the corresponding payoffs achieved by the players for certain strategies. The game is then said to be in strategic form. The players of our game are the transmitters, BS_1 and BS_2, and are to be referred to with their subscripts. The strategy of a player is his power allocation in each of his two bands. We define π_i, $0 \leq \pi_i \leq 1$, as the pure strategy of player i. Player 1 allocates $\pi_1 P$ in his protected band and $(1 - \pi_1)P$ in the shared band. Player 2, on the contrary, allocates $\pi_2 P$ in the shared band and $(1 - \pi_2)P$ in his protected band. This is the order reversing trick on the strategies of the players in order for the game, as is shown in the following section, to have strategic complementarities. Note that the applied trick does not work for more than two players. The payoff of a player is expressed in his utility function. We define the utility function of a player as his instantaneous achievable rate at his corresponding receiver. For a given strategy profile (π_1, π_2), the rate for the first system pair is formulated

Digital Object Identifier: 10.4108/ICST.VALUETOOLS2009.7793
http://dx.doi.org/10.4108/ICST.VALUETOOLS2009.7793

as

$$R_1(\pi_1,\pi_2) = \underbrace{\log_2(1+\rho\pi_1\alpha_1)}_{\text{Protected band}} + \underbrace{\log_2\left(1+\frac{\rho(1-\pi_1)\beta_{11}}{1+\rho\pi_2\beta_{21}}\right)}_{\text{Shared band}}, \quad (1)$$

and similarly for the second player as

$$R_2(\pi_1,\pi_2) = \log_2(1+\rho(1-\pi_2)\alpha_2) + \log_2\left(1+\frac{\rho\pi_2\beta_{22}}{1+\rho(1-\pi_1)\beta_{12}}\right), \quad (2)$$

where the transmitters are assumed to use random Gaussian codebooks and the interference at the receivers is treated as additive noise. The game is written as

$$G = \langle\{1,2\},([0,1],[0,1]),(R_1,R_2)\rangle. \quad (3)$$

This game is a non-cooperative static game in that the two players do not cooperate for choosing their strategies and each player is to decide for one strategy once and for all. The players are considered to be rational in that they strive to maximize their payoffs. The outcome of the game is a NE or a set of NEs. A NE is a strategy profile, $(\pi_1^{\text{NE}},\pi_2^{\text{NE}})$, in which no player can increase his payoff in deviating, choosing another strategy other than the NE strategy, unilaterally, i.e.

$$R_1(\pi_1^{\text{NE}},\pi_2^{\text{NE}}) \geq R_1(\pi_1',\pi_2^{\text{NE}}), \quad \text{for all } \pi_1' \in [0,1].$$

The formulation is written similarly for player 2.

3. NON-COOPERATIVE GAME

In this section, we analyze the non-cooperative spectrum sharing game in (3). That is, we characterize the existence, uniqueness and efficiency of the NEs. We relate this game to a class of non-cooperative games called supermodular games. These type of games have several properties that are relevant for our analysis.

3.1 Supermodular Games

Supermodular games are non-cooperative games where a player desires to increase his strategy as a response to an increase in the strategy of the other players. This situation exists due to the supermodularity of the players' utility function and the complementarity of their strategies.

DEFINITION 1 (SUPERMODULAR GAME [18]). *A non-cooperative game $S = \langle N,(A_i)_{i\in N},(R_i)_{i\in N}\rangle$ is a supermodular game if the following conditions are satisfied for each player $i \in N$:*

C1 *The set A_i of single dimensional feasible strategies is a compact set.*

C2 *The payoff function[1] $R_i(\pi_i,\pi_{-i})$ is upper semi continuous and has increasing differences in (π_i,π_{-i}) on $A_i \times A_{-i}$.*

For a more general definition of supermodular games in multi-dimensional strategies, refer to [19, p. 178]. Furthermore, application of supermodular games on wireless networks has been done in [20, 21].

[1]The subscript $-i$ denotes all players except player i.

LEMMA 1. *The game G defined in* (3) *is a supermodular game.*

PROOF. We prove that the game G satisfies the conditions $C1$ and $C2$. The first condition is satisfied because the strategy space $[0,1]$ is compact. Second, the utility functions in (1) and (2) are continuous which satisfies the first part of property $C2$. The second part of the property can be proven by showing

$$\frac{\partial^2 R_i(\pi_1,\pi_2)}{\partial\pi_1\partial\pi_2} \geq 0, \quad i = 1,2. \quad (4)$$

This is fulfilled since

$$\frac{\partial^2 R_1(\pi_1,\pi_2)}{\partial\pi_1\partial\pi_2} = \frac{\rho^2\beta_{21}\beta_{11}}{(1+\rho\pi_2\beta_{21}+\rho(1-\pi_1)\beta_{11})^2} \geq 0, \quad (5)$$

and

$$\frac{\partial^2 R_2(\pi_1,\pi_2)}{\partial\pi_1\partial\pi_2} = \frac{\rho^2\beta_{12}\beta_{22}}{(1+\rho\pi_2\beta_{22}+\rho(1-\pi_1)\beta_{12})^2} \geq 0. \quad (6)$$

Hence, the game G is a supermodular game. □

Supermodular games have several interesting properties. A few properties that are relevant to the case at hand are:

A1 There exists at least one pure strategy NE in the game [19, Theorem 4.2.1].

A2 The set of NEs is a complete lattice and there exist a largest element and a least element [19, Theorem 4.2.1].

A3 A unique NE is globally stable [22, Result 4].

A4 If the utility of a player is increasing in the strategies of the other players, then the largest (resp. smallest) equilibrium is the player's Pareto best (resp. worst) equilibrium [22, Result 3].

According to A1, the game G has at least one NE. From A3 follows that the uniqueness on NE implies convergence of the IWF from all strategy points. Therefore, we analyze next the uniqueness of the NE.

3.2 Uniqueness of Nash Equilibrium

The analysis for the uniqueness of the NE in a game can be done by studying the reaction curves of the players. Note that a similar characterization of the uniqueness of the NE is done in [9] for the more general interference relay scenario. HEre, we give a simpler and geometric derivation as well as a comparison with sufficient conditions for convergence of best response dynamics to NE.

The *reaction curve* $l_i : [0,1] \to [0,1]$ of a player i is a function that relates the strategy of player j, $j \neq i$, to the best response of player i in case the best response is a singleton [17]. The *best response* of a player is the strategy or set of strategies that maximize his utility function for a given strategy of the other player. For player 1, the best response to π_2 is unique and written as

$$br_1(\pi_2) = \arg\max_{\pi_1\in[0,1]} R_1(\pi_1,\pi_2). \quad (7)$$

A NE strategy profile consists of mutual best responses, i.e. $\pi_i^{\text{NE}} = br_i(\pi_{-i}^{\text{NE}})$. The player's utility function is concave in

Digital Object Identifier: 10.4108/ICST.VALUETOOLS2009.7793
http://dx.doi.org/10.4108/ICST.VALUETOOLS2009.7793

his own strategy since the second partial derivative of R_i with respect to $\pi_i, i = 1, 2$ is negative for all π_i

$$\frac{\partial^2 R_1(\pi_1,\pi_2)}{\partial^2 \pi_1} = -\left(\frac{\rho\alpha_1}{1+\rho\pi_1\alpha_1}\right)^2 - \left(\frac{\rho\beta_{11}}{1+\rho\pi_2\beta_{21}+\rho(1-\pi_1)\beta_{11}}\right)^2 < 0. \quad (8)$$

Therefore, the best response is given as the unique zero of the first derivative. For player 1, the partial derivative is calculated as

$$\frac{\partial R_1(\pi_1,\pi_2)}{\partial \pi_1} = \frac{\rho\alpha_1}{1+\rho\pi_1\alpha_1} - \frac{\rho\beta_{11}}{1+\rho\pi_2\beta_{21}+\rho(1-\pi_1)\beta_{11}}, \quad (9)$$

and set to zero to calculate the reaction curve function

$$l_1(\pi_2) = \left[\frac{1}{2} + \frac{\alpha_1-\beta_{11}}{2\alpha_1\rho\beta_{11}} + \frac{\beta_{21}\pi_2}{2\beta_{11}}\right]_0^1, \quad \pi_2 \in [0,1], \quad (10)$$

where $[x]_0^1$ represents the Euclidean projection of x on the interval $[0, 1]$. These bounds are required because the strategy space of a player is constrained to $[0, 1]$. The reaction curve $l_2(\pi_1)$ is similarly calculated for the second player as

$$l_2(\pi_1) = \left[\frac{1}{2} - \frac{\alpha_2-\beta_{22}+\beta_{12}\alpha_2\rho}{2\alpha_2\rho\beta_{22}} + \frac{\beta_{12}\pi_1}{2\beta_{22}}\right]_0^1, \quad (11)$$

where $\pi_1 \in [0, 1]$. The reaction curves in a supermodular game are monotonic due to the complementarity relationship between the strategies of the players. An intersection point of the reaction curves, $l_1(\pi_2)$ and $l_2(\pi_1)$, consists of mutual best responses which would be a NE strategy profile. Hence, the number of intersections of the curves is the number of NEs in the game. Next, we analyze the reaction curves neglecting the bounds as in (10) and (11). For convenience, we define an *unbounded reaction curve* as

$$l_1'(\pi_2) = \frac{1}{2} + \frac{\alpha_1-\beta_{11}}{2\alpha_1\rho\beta_{11}} + \frac{\beta_{21}\pi_2}{2\beta_{11}}, \quad \pi_2 \in [0,1], \quad (12)$$

for the first player, and similarly $l_2'(\pi_1)$ is the unbounded reaction curve for player 2,

$$l_2'(\pi_1) = \frac{1}{2} - \frac{\alpha_2-\beta_{22}+\beta_{12}\alpha_2\rho}{2\alpha_2\rho\beta_{22}} + \frac{\beta_{12}\pi_1}{2\beta_{22}}, \quad \pi_1 \in [0,1]. \quad (13)$$

The intersection point of the unbounded reaction curves of the two players is denoted as (π_1^*, π_2^*) given by

$$\pi_1^* = \frac{2\beta_{11}\beta_{22} + \frac{2\beta_{22}}{\rho} - \frac{2\beta_{11}\beta_{22}}{\alpha_1\rho}}{4\beta_{11}\beta_{22}-\beta_{12}\beta_{21}} + \frac{\beta_{21}\beta_{22} - \frac{\beta_{21}}{\rho} + \frac{\beta_{21}\beta_{22}}{\alpha_2\rho} - \beta_{12}\beta_{21}}{4\beta_{11}\beta_{22}-\beta_{12}\beta_{21}}, \quad (14)$$

$$\pi_2^* = \frac{2\beta_{11}\beta_{22} - \frac{2\beta_{11}}{\rho} + \frac{2\beta_{11}\beta_{22}}{\alpha_2\rho}}{4\beta_{11}\beta_{22}-\beta_{12}\beta_{21}} - \frac{\beta_{12}\beta_{11} - \frac{\beta_{12}}{\rho} + \frac{\beta_{12}\beta_{11}}{\alpha_1\rho}}{4\beta_{11}\beta_{22}-\beta_{12}\beta_{21}}. \quad (15)$$

For the case that $\beta_{12}\beta_{21} = 4\beta_{11}\beta_{22}$, the unbounded reaction curves are parallel, and hence they either overlap or do not intersect.

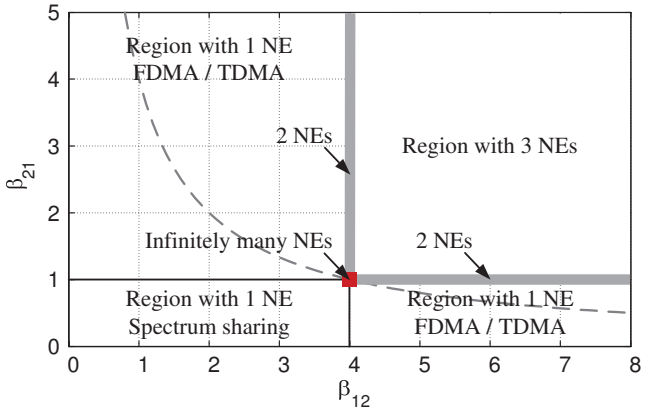

Figure 3: Interference regions for $\rho = 0$ dB, $\alpha_1 = 2$, $\alpha_2 = 1, \beta_{11} = 1, \beta_{22} = 1$. The dashed curve corresponds to $\beta_{12}\beta_{21} = 4$.

PROPOSITION 1. *A sufficient condition for the existence of a unique NE is that $\beta_{12}\beta_{21} < 4\beta_{11}\beta_{22}$.*

PROOF. See Appendix 5.1. □

In Fig. 3, the sufficient condition for the existence of a unique NE corresponds to the region below the dashed line. The area marked with spectrum sharing resembles the area where the NE lies in the strategy region. There only adaptive spectrum sharing is used. According to property A4, Proposition 1 states the sufficient condition for the convergence of the best response dynamics. These dynamics can have an asynchronous update policy [23, Theorem 8]. In [15], a unified framework is given for the analysis of the convergence of the IWF. According to our system model, the sufficient conditions for the convergence of the asynchronous IWF in that work corresponds to $\beta_{12}\beta_{21} < \beta_{11}\beta_{22}$. Hence, the condition in Proposition 1 leads to a larger region of convergence.

PROPOSITION 2. *There exist infinitely many NEs if and only if the following conditions are satisfied:*

(a) The unbounded reaction curves are parallel, i.e.

$$\beta_{12}\beta_{21} = 4\beta_{11}\beta_{22}.$$

(b) The reaction curves lie on one line, i.e.

$$\beta_{12} = 2\beta_{11}\frac{\frac{\beta_{22}}{\alpha_2}+\rho\beta_{22}-1}{\frac{\beta_{11}}{\alpha_1}+\rho\beta_{11}-1}.$$

(c) The reaction curves pass the region $[0, 1]^2$ simultaneously, i.e.

$$\{\alpha_1(1-\rho\beta_{11})-\beta_{11}<0\} \wedge \{\alpha_2(1-\rho\beta_{22})-\beta_{22}<0\} \wedge \left\{\beta_{21} > \frac{\beta_{11}-\alpha_1(\rho\beta_{11}+1)}{\alpha_1\rho}\right\} \wedge \left\{\beta_{12} > \frac{\beta_{22}-\alpha_2(\rho\beta_{22}+1)}{\alpha_2\rho}\right\}.$$

PROOF. See Appendix 5.2. □

Digital Object Identifier: 10.4108/ICST.VALUETOOLS2009.7793
http://dx.doi.org/10.4108/ICST.VALUETOOLS2009.7793

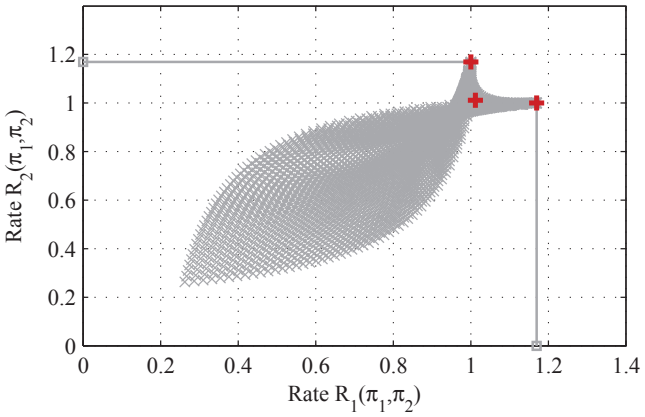

Figure 4: Rate region for $\rho = 0$ dB, $\alpha_1 = 1$, $\alpha_2 = 1$, $\beta_{11} = 1$, $\beta_{22} = 1$, $\beta_{12} = 4$, $\beta_{21} = 4$. Three NEs exist and are marked with a red plus.

When infinitely many NEs exist, two NEs lie on the boundary of the strategy region. According to property A4, each NE of these two is the Pareto best NE for one player and worst for the other player. In general, no NE of the infinitely many NEs dominates all others.

COROLLARY 1. *There exists a unique NE if $\beta_{12}\beta_{21} = 4\beta_{11}\beta_{22}$ and if at least one of the conditions (b) or (c) of Proposition 2 is not satisfied.*

The region induced by this corollary is the dashed line in Fig. 3 without the red square, and the unique NE for this case lies on the boundary of the strategy region.

PROPOSITION 3. *For $\beta_{12}\beta_{21} > 4\beta_{11}\beta_{22}$, there exists a unique NE if and only if $(\pi_1^*, \pi_2^*) \notin [0,1]^2$.*

PROOF. See Appendix 5.3. □

In Proposition 3, the NE lies also on the boundary of the region $[0,1]^2$. In the case that multiple NEs exist, property A4 describes the equilibria in their efficiency for each player. An example is given in Fig. 4 where three NEs exist. The NE rate pair inside the region corresponds to the NE strategy profile inside $[0,1]^2$. Based on this observation, the entire interference region where $\beta_{12}\beta_{21} \geq 4\beta_{11}\beta_{22}$ suits best for orthogonal resource allocation as FDMA/TDMA. In Fig. 3, the regions are illustrated.

3.3 Probability of Spectrum Sharing

Utilities R_1 and R_2 are random variables because α_1, α_2 and $\beta_{11}, \beta_{12}, \beta_{21}, \beta_{22}$ are fading channels. Now, we assume that the channels are quasi-static block flat-fading and compute the probability of spectrum sharing. Spectrum sharing is done when both base stations use the shared band simultaneously. This is equivalent to the case that the NE lies in the strategy region $[0,1) \times (0,1]$. In this section, we calculate the probability of spectrum sharing for specific channel gains distributions. For simplicity we choose $\rho = 0$ dB and $\beta_{11} = \beta_{22} = 1$. The conditions that the NE lies inside the region $[0,1) \times (0,1]$ are then given as

$$\beta_{12}\beta_{21} < 4 \text{ and } \beta_{12} < 2\frac{\alpha_1}{\alpha_2}. \tag{16}$$

Hence, the probability of spectrum sharing is equivalent to

$$\Pr\left[\frac{\beta_{12}}{2} < \frac{\alpha_1}{\alpha_2} < \frac{2}{\beta_{21}}\right]. \tag{17}$$

Table 1 shows the results for the following channel distributions. The direct coefficients, α_1 and α_2, are independently and identically standard exponentially distributed random variables. The cross channels coefficients, β_{12} and β_{21}, are also independently and identically exponentially distributed with mean varied as in the table. The results show that the probability that the shared band is simultaneously used by the non-cooperative systems is relatively large, which acknowledges the utility of the protected and shared bands scenario.

Distribution mean of β_{12} and β_{21}	Probability of spectrum sharing
0.2	0.83
0.3	0.76
0.4	0.70
0.5	0.65
0.6	0.60
0.7	0.55

Table 1: Probability of spectrum sharing for different distribution mean of the cross channel coefficients.

3.4 Average Sum Rates

In this section, we analyze the average sum rates achieved on non-cooperation in the protected and shared bands scenario in comparison to three other settings. In the first setting, we allow cooperation of the base stations in the same scenario of protected and shared bands. In the second setting, the base stations use only protected bands each. In the third setting, the base stations share all the available spectrum non-cooperatively. For each scenario, six independent bands are available and these are arranged to BS_1 and BS_2 as illustrated in Fig. 5.

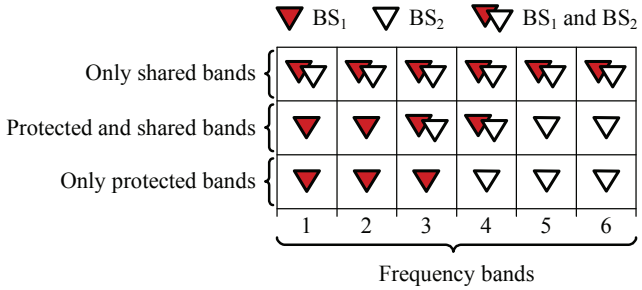

Figure 5: Illustration of the frequency bands assignments for the three settings.

On non-cooperation in the protected and shared bands case, the systems operate on the NE strategy to achieve an

Digital Object Identifier: 10.4108/ICST.VALUETOOLS2009.7793
http://dx.doi.org/10.4108/ICST.VALUETOOLS2009.7793

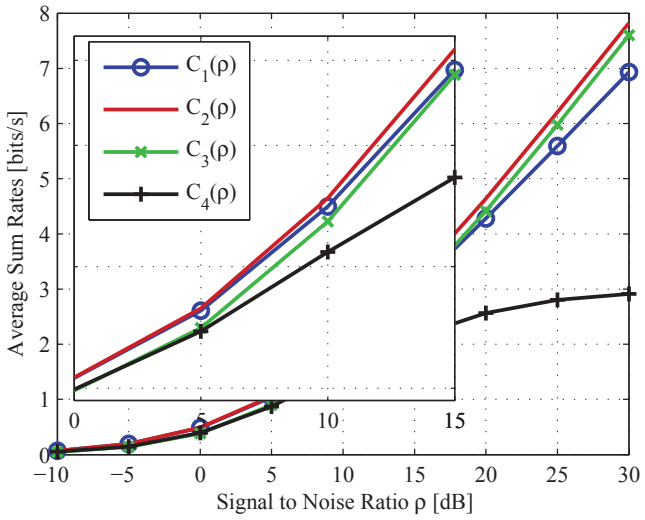

Figure 6: Comparison of achievable average sum rates. The mean for the direct channel coefficients is one and SIR is 0dB.

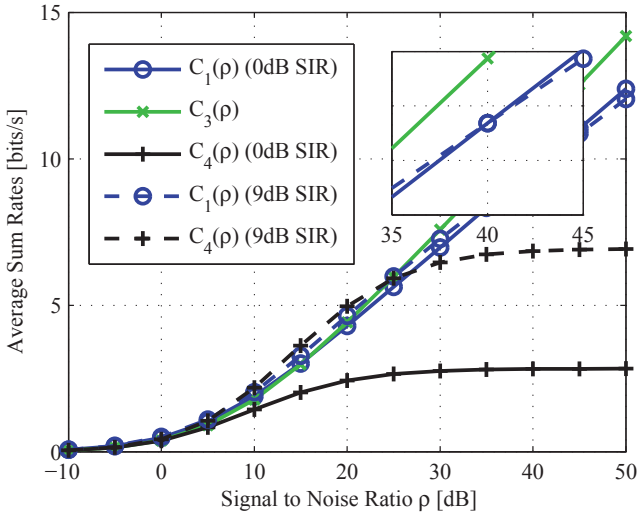

Figure 7: Comparison of achievable average sum rates for increasing SIR. The mean for the direct channel coefficients is one.

average sum rate of

$$C_1(\rho) = \frac{1}{6}\mathbb{E}\Bigg[2\log_2\left(1+\frac{\rho}{2}\pi_1^{\mathrm{NE}}\alpha_1\right) + 2\log_2\left(1+\frac{\frac{\rho}{2}(1-\pi_1^{\mathrm{NE}})\beta_{11}}{1+\frac{\rho}{2}\pi_2^{\mathrm{NE}}\beta_{21}}\right) + 2\log_2\left(1+\frac{\rho}{2}(1-\pi_2^{\mathrm{NE}})\alpha_2\right) + 2\log_2\left(1+\frac{\frac{\rho}{2}\pi_2^{\mathrm{NE}}\beta_{22}}{1+\frac{\rho}{2}(\pi_1^{\mathrm{NE}})\beta_{12}}\right)\Bigg], \quad (18)$$

where the expectation is with respect to α_1, α_2, β_{11}, β_{12}, β_{21}, and β_{22}. Note that the NE strategies depend on these parameters, i.e. π_1^{NE} and π_2^{NE} are functions of α_1, α_2, β_{11}, β_{12}, β_{21}, and β_{22}. When multiple NEs exist, the least efficient one is chosen. For the cooperative case, the systems operate on the strategy profile that achieves the maximum sum rate. The average maximum sum rate for this case is written as

$$C_2(\rho) = \frac{1}{6}\mathbb{E}\Bigg[\max_{\pi_1,\pi_2\in[0,1]}\Bigg(2\log_2\left(1+\frac{\rho}{2}\pi_1\alpha_1\right) + 2\log_2\left(1+\frac{\frac{\rho}{2}(1-\pi_1)\beta_{11}}{1+\frac{\rho}{2}\pi_2\beta_{21}}\right) + 2\log_2\left(1+\frac{\rho}{2}(1-\pi_2)\alpha_2\right) + 2\log_2\left(1+\frac{\frac{\rho}{2}\pi_2\beta_{22}}{1+\frac{\rho}{2}(\pi_1)\beta_{12}}\right)\Bigg)\Bigg], \quad (19)$$

where the expectation is with respect to $\alpha_1, \alpha_2, \beta_{11}, \beta_{12}, \beta_{21}$, and β_{22}. For the scenario of only protected bands, the average sum rates is given as

$$C_3(\rho) = \frac{1}{6}\mathbb{E}\left[3\log_2\left(1+\frac{\rho}{3}\alpha_1\right) + 3\log_2\left(1+\frac{\rho}{3}\alpha_2\right)\right], \quad (20)$$

where the expectation is with respect to α_1 and α_2. For the only shared bands case, the non-cooperative case is chosen for which the systems spread their powers over all bands. The average sum rates are hence calculated as

$$C_4(\rho) = \frac{1}{6}\mathbb{E}\Bigg[6\log_2\left(1+\frac{\frac{\rho}{6}\beta_{11}}{1+\frac{\rho}{6}\beta_{21}}\right) + 6\log_2\left(1+\frac{\frac{\rho}{6}\beta_{22}}{1+\frac{\rho}{6}\beta_{12}}\right)\Bigg], \quad (21)$$

where the expectation is with respect to $\beta_{11}, \beta_{12}, \beta_{21}$, and β_{22}. All channel coefficients are independently exponentially distributed with different mean.

The performance of the three settings is shown in Fig. 6. The average receive signal to interference ratio (SIR) is defined as

$$\mathrm{SIR} = \frac{\mathbb{E}[\beta_{ii}]}{\mathbb{E}[\beta_{ji}]}, \quad i \neq j.$$

The cooperative case in the protected and shared bands achieves the highest performance. In comparison to the only protected bands case, the increase in performance results due to the multiuser diversity effect [24, Chapter 6]. The sum rates are maximized through opportunistic scheduling, which in our case corresponds to choosing the mobile station with the strongest channel for transmission in the shared band.

The non-cooperative case in the protected and shared bands is first compared to that of the cooperative case. For increasing SNR, the curves that are overlapping in the low SNR regime become distinct with increasing gap. This degradation in performance due to non-cooperation of the systems is explained in the next section.

In Fig. 7, we show the performance of the systems on varying the SIR. Increasing the SIR increases the performance of the only shared bands case. For the protected and shared bands case, we observe the following. In the low and medium SNR regimes, the performance of the system increases. In the high SNR regime, on the contrary, a degradation in performance occurs. This result is an investigation for future work.

Digital Object Identifier: 10.4108/ICST.VALUETOOLS2009.7793
http://dx.doi.org/10.4108/ICST.VALUETOOLS2009.7793

3.5 Efficiency of Nash Equilibria

The Price of Anarchy (PoA) [25,26] is a quantitative measure of efficiency of a non-cooperative system. Knowing that the maximum achievable payoffs for both players are reached on cooperation, the PoA is defined as the ratio of the maximum achievable sum utilities of the players cooperating, U_{OPT}, over the sum utilities of their worst case NE, U_{NE}. The PoA is written as

$$\text{PoA} = \frac{U_{\text{OPT}}}{U_{\text{NE}}}. \tag{22}$$

PROPOSITION 4. *The PoA of our system is upper bounded by*

$$\begin{aligned} PoA \leq 1 + \frac{\log_2(1+\rho(|\beta_{11}|^2+|\beta_{12}|^2))}{\log_2((1+\rho\alpha_1)(1+\rho\alpha_2))} \\ + \frac{\log_2(1+\rho(|\beta_{22}|^2+|\beta_{21}|^2))}{\log_2((1+\rho\alpha_1)(1+\rho\alpha_2))}. \end{aligned} \tag{23}$$

PROOF. The proof is given in [10, Section V.B][2]. □

The PoA is plotted as a function of the SNR in Fig. 8. The plot explains the results on the efficiency of the non-cooperative setting in the previous section. For low SNR, the PoA is one which reveals that the efficiency of the system on non-cooperation is the same as on cooperation in that regime. However, the PoA increases with increasing SNR which explains the increasing gap between the curves in Fig. 6. In the next section, an asymptotic analysis on the efficiency of the system is made for high SNR.

3.5.1 Efficiency at High SNR

The quantitative performance is analyzed using the high-SNR offset concept in [27, Section II]. Denote as $C(\rho)$ the sum rate as a function of the SNR. The two high-SNR measures are introduced as follows

$$S_\infty = \lim_{\rho\to\infty} \frac{C(\rho)}{\log_2(\rho)} \quad \text{and} \tag{24}$$

$$L_\infty = \lim_{\rho\to\infty} \left(\log_2(\rho) - \frac{C(\rho)}{S_\infty} \right). \tag{25}$$

The measure S_∞ is called high-SNR slope and the measure L_∞ is called high-SNR power offset. At high SNR the sum rate behaves like

$$C(\rho) = S_\infty \left(\frac{\rho[dB]}{3dB} - L_\infty \right) + \mathcal{O}(1). \tag{26}$$

These two high SNR measures are useful if two systems are compared which differ either in their multiplexing gain, i.e. the slope of the sum rate curve at high SNR, or which have equal S_∞ but have shifted rate curves at high SNR.

LEMMA 2. *The high-SNR slope of the sum rates is maximum, $S_\infty = 1$, when*

$$\pi_1 = 1 \text{ and } 0 < \pi_2 < 1$$

or

$$0 < \pi_1 < 1 \text{ and } \pi_2 = 0.$$

[2]The bound in the reference is calculated for $\beta_{11} = \beta_{22} = 1$. The calculations, however, can be easily adapted to include β_{11} and β_{22}.

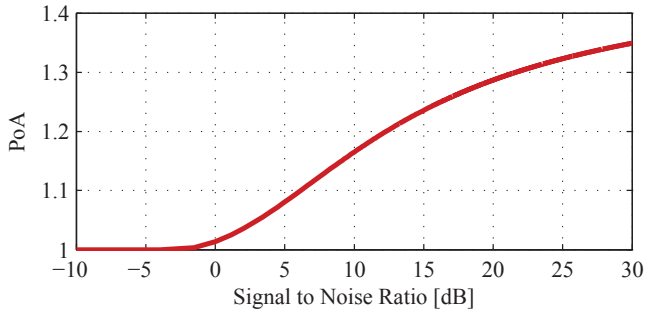

Figure 8: PoA for increasing average SNR ($\alpha_1 = 2$, $\alpha_2 = 2$, $\beta_{11} = 1$, $\beta_{22} = 1$, $\beta_{12} = 3$, $\beta_{21} = 5$).

PROOF. See Appendix 5.4. □

The strategies in Lemma 2 correspond to one player using only its protected band and the other player using both its protected and the shared band. This result is useful to come to the following proposition.

PROPOSITION 5. *The maximum achievable sum rate, U_{OPT}, at high SNR corresponds to the strategy profile*

$$(\pi_1^{OPT}, \pi_2^{OPT}) = \begin{cases} (1, \frac{1}{2}) & \text{if} \quad \beta_{11} < \beta_{22} \\ (\frac{1}{2}, 0) & \text{if} \quad \beta_{11} > \beta_{22} \end{cases}. \tag{27}$$

PROOF. See Appendix 5.5 □

The result in Proposition 5 reflects which strategy the systems would choose on cooperation in order to maximize the sum rates. Following are the results that characterize the high-SNR measures when operating in the NE strategy, i.e. on non-cooperation of the systems.

LEMMA 3. *For $\rho \to \infty$, the worst case NE achieves sum rate, U_{NE}, with*

$$S_\infty \geq \frac{2}{3}.$$

PROOF. See Appendix 5.6. □

Using the analysis of the sum rates for the cooperative and non-cooperative settings, the PoA at high SNR can be studied.

PROPOSITION 6. *The PoA for $\rho \to \infty$ is bounded such that*

$$PoA = \lim_{\rho\to\infty} \frac{U_{OPT}}{U_{NE}} \leq \frac{3}{2}. \tag{28}$$

PROOF. See Appendix 5.7. □

In other words, at high SNR the efficiency of the system operating non-cooperatively can not be worse than $\frac{2}{3}$ the efficiency of a cooperating system. This result is in contrast to [28] where the PoA grows unbounded with SNR.

4. CONCLUSION

We study the existence, uniqueness, and efficiency of the NE in a system utilizing protected and shared bands. The uniqueness conditions are proven to satisfy the global convergence of the IWF algorithm. Moreover, these conditions

Digital Object Identifier: 10.4108/ICST.VALUETOOLS2009.7793
http://dx.doi.org/10.4108/ICST.VALUETOOLS2009.7793

refer to interference regions that include the sufficient conditions for convergence of the IWF found in the literature. Hence, a larger region is shown to exist that satisfies the convergence of the algorithm. Next, we show that for low interference the probability that the protected and shared bands setting is used by the non-cooperative system pairs is high. This leads us to investigate the efficiency of this setting. We compare the spectral efficiency of the system to that of the scenarios where only protected bands or only shared bands are used. The combination of protected and shared bands gives higher performance than the only protected bands in the low SNR regimes and higher performance than the only shared bands in the high SNR regime. Regarding the efficiency of the non-cooperative system, we show that with increasing SNR the PoA is bounded by a value of $\frac{3}{2}$.

A future work is to develop a method to compute the sets of NEs and their efficiency to one another. An investigation whether the IWF is globally convergent for the case that the NE is not unique is to be done. Furthermore, the system model will be extended to the more general case. The scenario will have multiple cells. The base stations and mobiles are to be equipped with multiple antennas.

5. APPENDIX

5.1 Proof of Proposition 1

In the case that $\beta_{12}\beta_{21} < 4\beta_{11}\beta_{22}$, the unbounded reaction curves, $l_1'(\pi_2)$ and $l_2'(\pi_1)$, would intersect in one point. Whether this intersection point is inside or outside the region $[0,1]^2$, two cases are to be studied. If $(\pi_1^*, \pi_2^*) \in [0,1]^2$, this intersection point would be a unique NE due to condition $\beta_{12}\beta_{21} < 4\beta_{11}\beta_{22}$ for which the slopes of the curves to one another satisfies that the bounded reaction curves do not intersect on another point on the boundary. This condition is illustrated in Fig. 9 (a). For the case that $(\pi_1^*, \pi_2^*) \notin [0,1]^2$, the NE is unique and lies on the boundary of the region as illustrated in Fig. 9 (b).

5.2 Proof of Proposition 2

The proof is based on the observation of the arrangement of the reaction curves on the corresponding stated condition. In order that infinitely many NEs exist, it is necessary that the reaction curves lie over one another. The condition $\beta_{12}\beta_{21} = 4\beta_{11}\beta_{22}$ satisfies that the unbounded reaction curves, $l_1'(\pi_2)$ and $l_2'(\pi_1)$, be parallel. Secondly, the condition (b) of the proposition assures that the curves lie on one line which excludes the case as in Fig. 9 (c). The third condition (c) of the proposition excludes the case that both lines lie totaly outside the region which would lead to a single NE as in Fig. 9 (d). Therefore, the three conditions are necessary for the existence of infinitely many NEs as in Fig. 9 (e).

5.3 Proof of Proposition 3

The proof is based on the observation of the arrangement of the reaction curves on the corresponding stated condition. For the case $(\pi_1^*, \pi_2^*) \in (0,1)^2$, this intersection point is counted as a NE. The condition $\beta_{12}\beta_{21} > 4\beta_{11}\beta_{22}$ satisfies the reaction curves to intersect one another on two extra points on the boundary of the strategy region as illustrated in Fig. 9 (f). If (π_1^*, π_2^*) is on the boundary of the region $[0,1]^2$, then it is counted as a NE and a second NE exists on the other boundary as in Fig. 9 (g).

5.4 Proof of Lemma 2

In order to find the maximum high-SNR slope of the sum rate, we calculate the value of the slope for all possible cases of the strategies of the players. The sum rate as a function of SNR is written as

$$\begin{aligned} C(\rho) &= \frac{1}{3}\left(R_1(\pi_1,\pi_2) + R_2(\pi_1,\pi_2)\right) \\ &= \frac{1}{3}\Bigg(\log_2(1+\rho\pi_1\alpha_1) \\ &\quad + \log_2(1+\rho(1-\pi_2)\alpha_2) \\ &\quad + \log_2\left(1+\frac{\rho(1-\pi_1)\beta_{11}}{1+\rho\pi_2\beta_{21}}\right) \\ &\quad + \log_2\left(1+\frac{\rho\pi_2\beta_{22}}{1+\rho(1-\pi_1)\beta_{12}}\right)\Bigg). \end{aligned} \tag{29}$$

The high-SNR slope of the sum rate defined in (24) is calculated as

$$\begin{aligned} S_\infty = \frac{1}{3}\Bigg(&\lim_{\rho\to\infty}\frac{\log_2(1+\rho\pi_1\alpha_1)}{\log_2(\rho)} \\ &+ \lim_{\rho\to\infty}\frac{\log_2(1+\rho(1-\pi_2)\alpha_2)}{\log_2(\rho)} \\ &+ \lim_{\rho\to\infty}\frac{\log_2\left(1+\rho(1-\pi_1)\beta_{11}+\rho\pi_2\beta_{21}\right)}{\log_2(\rho)} \\ &- \lim_{\rho\to\infty}\frac{\log_2\left(1+\rho\pi_2\beta_{21}\right)}{\log_2(\rho)} \\ &+ \lim_{\rho\to\infty}\frac{\log_2\left(1+\rho(1-\pi_1)\beta_{12}+\rho\pi_2\beta_{22}\right)}{\log_2(\rho)} \\ &- \lim_{\rho\to\infty}\frac{\log_2\left(1+\rho(1-\pi_1)\beta_{12}\right)}{\log_2(\rho)}\Bigg). \end{aligned} \tag{30}$$

All nine possible cases on the players' strategies are stated in Table 2 with the corresponding S_∞.

Cases	Strategy player 1	Strategy player 2	S_∞
1.	$\pi_1 = 1$	$\pi_2 = 0$	$\frac{2}{3}$
2.	$\pi_1 = 1$	$\pi_2 = 1$	$\frac{2}{3}$
3.	$\pi_1 = 1$	$0 < \pi_2 < 1$	1
4.	$\pi_1 = 0$	$\pi_2 = 0$	$\frac{2}{3}$
5.	$\pi_1 = 0$	$\pi_2 = 1$	0
6.	$\pi_1 = 0$	$0 < \pi_2 < 1$	$\frac{1}{3}$
7.	$0 < \pi_1 < 1$	$\pi_2 = 0$	1
8.	$0 < \pi_1 < 1$	$\pi_2 = 1$	$\frac{1}{3}$
9.	$0 < \pi_1 < 1$	$0 < \pi_2 < 1$	$\frac{2}{3}$

Table 2: Values of S_∞ for all relevant combinations of the players' strategies.

The highest value of the slope as shown in the table is $S_\infty^{\mathrm{OPT}} = 1$, which concludes the proof.

5.5 Proof of Proposition 5

For the case $\pi_1 = 1$ and $0 < \pi_2 < 1$, the high-SNR power offset of the sum rate in (25) is calculated as

Digital Object Identifier: 10.4108/ICST.VALUETOOLS2009.7793
http://dx.doi.org/10.4108/ICST.VALUETOOLS2009.7793

$$
\begin{aligned}
L_\infty(1,\pi_2) &= \lim_{\rho\to\infty}\Bigg(\log_2(\rho) - \frac{1}{3}\log_2(1+\rho\alpha_1) \\
&\quad + \frac{1}{3}\log_2(1+\rho(1-\pi_2)\alpha_2) \\
&\quad + \frac{1}{3}\log_2(1+\rho\pi_2\beta_{22})\Bigg) \\
&= \lim_{\rho\to\infty}\log_2\Bigg(\frac{\rho^2}{(1+\rho\alpha_1)} \\
&\quad \times \frac{1}{(1+\rho(1-\pi_2)\alpha_2)(1+\rho\pi_2\beta_{22})}\Bigg) \\
&= -\frac{1}{3}\log_2(\alpha_1\alpha_2\beta_{22}\pi_2(1-\pi_2)).
\end{aligned} \tag{31}
$$

The strategy that maximizes the sum rate at high SNR is the one that minimizes this distance. L_∞ is minimized for

$$
\pi_2^{\mathrm{OPT}} = \arg\min_{0<\pi_2<1} L_\infty(1,\pi_2) = \frac{1}{2}, \tag{32}
$$

and has a value of

$$
L_\infty\left(1,\frac{1}{2}\right) = -\frac{1}{3}\log_2\left(\frac{\alpha_1\alpha_2\beta_{22}}{4}\right). \tag{33}
$$

For $\pi_2 = 0$ and $0 < \pi_1 < 1$, the offset is calculated similarly and has a minimum for the strategy profile

$$
\pi_1^{\mathrm{OPT}} = \arg\min_{0<\pi_1<1} L_\infty(\pi_1,0) = \frac{1}{2}, \tag{34}
$$

with

$$
L_\infty\left(\frac{1}{2},0\right) = -\frac{1}{3}\log_2\left(\frac{\alpha_1\alpha_2\beta_{11}}{4}\right). \tag{35}
$$

The maximum sum rates corresponds to the strategy profile that leads to the least L_∞. In comparing (33) and (35), the conditions for choosing the sum rate maximizing strategy profile is dependent on the relation of β_{11} and β_{22} which lead to the result in (27).

5.6 Proof of Lemma 3

For the asymptotic case, $\rho \to \infty$, the reaction curves in (10) and (11) can be written as

$$
l_1(\pi_2) = \left[\frac{1}{2} + \frac{\beta_{21}\pi_2}{2\beta_{11}}\right]_0^1, \quad \pi_2 \in [0,1], \tag{36}
$$

and

$$
l_2(\pi_1) = \left[\frac{1}{2} + \frac{\beta_{12}}{2\beta_{22}}(1-\pi_1)\right]_0^1, \quad \pi_1 \in [0,1]. \tag{37}
$$

The minimum value that $l_1(\pi_2)$ can take is $\frac{1}{2}$ and the maximum value that $l_2(\pi_1)$ can take is $\frac{1}{2}$. Therefore, the NEs have to lie in the region $[\frac{1}{2},1]\times[0,\frac{1}{2}]$. The corresponding high-SNR slope of the sum rates for the strategies in this region are given in Table 3. Hence, the least value of the slope S_∞ is $\frac{2}{3}$, i.e. $S_\infty^{\mathrm{NE}} \geq \frac{2}{3}$.

5.7 Proof of Proposition 6

The sum rates for high SNR behave as in (26). Given the definition of PoA in (22) and using the asymptotic expansion

Cases	Strategy player 1	Strategy player 2	S_∞
1.	$\pi_1 = 1$	$\pi_2 = 0$	$\frac{2}{3}$
2.	$\pi_1 = 1$	$0 < \pi_2 < 1$	1
3.	$0 < \pi_1 < 1$	$\pi_2 = 0$	1
4.	$0 < \pi_1 < 1$	$0 < \pi_2 < 1$	$\frac{2}{3}$

Table 3: Values of S_∞ for all relevant combinations of the players' strategies in $[\frac{1}{2},1]\times[0,\frac{1}{2}]$.

from (26), we can write

$$
\begin{aligned}
\mathrm{PoA} &= \lim_{\rho\to\infty}\frac{U_{\mathrm{OPT}}}{U_{\mathrm{NE}}} \\
&= \lim_{\rho\to\infty}\frac{S_\infty^{\mathrm{OPT}}\left(\frac{\rho[dB]}{3dB} - L_\infty^{\mathrm{OPT}}\right) + \mathcal{O}(1)}{S_\infty^{\mathrm{NE}}\left(\frac{\rho[dB]}{3dB} - L_\infty^{\mathrm{NE}}\right) + \mathcal{O}(1)} \leq \frac{3}{2},
\end{aligned} \tag{38}
$$

where L_∞^{OPT} and L_∞^{NE} are the high-SNR power offsets for the maximum sum rate and the sum rate at NE respectively. For $\rho \to \infty$, the PoA has a maximum of $\frac{3}{2}$ which concludes the proof.

6. REFERENCES

[1] K. H. Teo, Z. Tao, and J. Zhang, "The mobile broadband WiMAX standard," *Signal Processing Magazine, IEEE*, vol. 24, no. 5, pp. 144–148, Sept. 2007.

[2] Y. Chen, W. Wang, T. Li, X. Zhang, and M. Peng, "Fractional frequency reuse in mobile WiMAX," *Communications and Networking in China, 2008. ChinaCom 2008. Third International Conference on*, pp. 276–280, Aug. 2008.

[3] R. Etkin, A. Parekh, and D. Tse, "Spectrum sharing for unlicensed bands," *Selected Areas in Communications, IEEE Journal on*, vol. 25, no. 3, pp. 517–528, Apr. 2007.

[4] L. Grokop and D. Tse, "Spectrum sharing between wireless networks," *INFOCOM 2008. The 27th Conference on Computer Communications. IEEE*, pp. 201–205, Apr. 2008.

[5] F. Meshkati, H. Poor, and S. Schwartz, "Energy-efficient resource allocation in wireless networks," *Signal Processing Magazine, IEEE*, vol. 24, no. 3, pp. 58–68, May 2007.

[6] M. Chiang, P. Hande, T. Lan, and C. W. Tan, "Power control in wireless cellular networks," *Found. Trends Netw.*, vol. 2, no. 4, pp. 381–533, 2008.

[7] A. Leshem and E. Zehavi, "Game theory and the frequency selective interference channel," *Signal Processing Magazine, IEEE*, Sept. 2009, will appear.

[8] M. Bennis, M. L. Treust, S. Lasaulce, M. Debbah, and J. Lilleberg, "Spectrum sharing games on the interference channel," in *International Conference on Game Theory for Networks (GameNets)*, Istanbul, Turkey, May 2009.

[9] E. Belmega, B. Djeumou, and S. Lasaulce, "Resource allocation games in interference relay channels," in *Game Theory for Networks, 2009. GameNets '09. International Conference on*, May 2009, pp. 575–584.

[10] E. Jorswieck and R. Mochaourab, "Power control game in protected and shared bands: Manipulability of Nash equilibrium," in *International Conference on*

Digital Object Identifier: 10.4108/ICST.VALUETOOLS2009.7793
http://dx.doi.org/10.4108/ICST.VALUETOOLS2009.7793

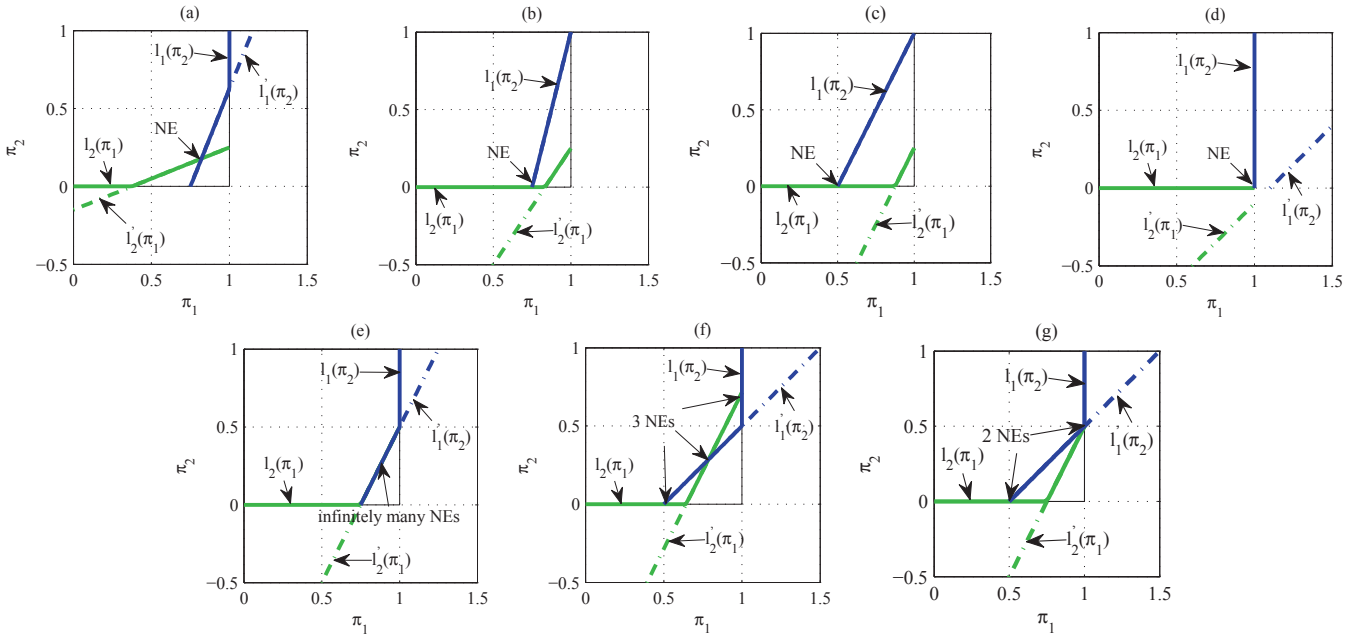

Figure 9: Illustration of the arrangement of the reaction curves.

Game Theory for Networks (GameNets), Istanbul, Turkey, May 2009, invited.

[11] W. Yu, G. Ginis, and J. Cioffi, "Distributed multiuser power control for digital subscriber lines," *Selected Areas in Communications, IEEE Journal on*, vol. 20, no. 5, pp. 1105–1115, June 2002.

[12] S. T. Chung, S. J. Kim, J. Lee, and J. Cioffi, "A game-theoretic approach to power allocation in frequency-selective Gaussian interference channels," *Information Theory, 2003. Proceedings. IEEE International Symposium on*, pp. 316–316, June 2003.

[13] K. Shum, K.-K. Leung, and C. W. Sung, "Convergence of iterative waterfilling algorithm for Gaussian interference channels," *Selected Areas in Communications, IEEE Journal on*, vol. 25, no. 6, pp. 1091–1100, Aug. 2007.

[14] Z.-Q. Luo and J.-S. Pang, "Analysis of iterative waterfilling algorithm for multiuser power control in digital subscriber lines," *EURASIP Journal on Applied Signal Processing*, vol. 2006, no. 1, p. 10 Pages, 2006.

[15] G. Scutari, D. Palomar, and S. Barbarossa, "Competitive design of multiuser MIMO systems based on game theory: A unified view," *Selected Areas in Communications, IEEE Journal on*, vol. 26, no. 7, pp. 1089–1103, Sept. 2008.

[16] J. Zander, "Distributed cochannel interference control in cellular radio systems," *Vehicular Technology, IEEE Transactions on*, vol. 41, no. 3, pp. 305–311, Aug. 1992.

[17] T. Basar and G. J. Olsder, *Dynamic Noncooperative Game Theory (Classics in Applied Mathematics, 23)*. Soc for Industrial & Applied Math, December 1998.

[18] R. Amir, "Supermodularity and complementarity in economics: An elementary survey," *Southern Economic Journal*, vol. 71, no. 3, pp. 636–660, Jan. 2005.

[19] D. M. Topkis, *Supermodularity and Complementarity*. Princeton University Press, 1998.

[20] C. Saraydar, N. Mandayam, and D. Goodman, "Efficient power control via pricing in wireless data networks," *Communications, IEEE Transactions on*, vol. 50, no. 2, pp. 291–303, Feb. 2002.

[21] E. Altman and Z. Altman, "S-modular games and power control in wireless networks," *Automatic Control, IEEE Transactions on*, vol. 48, no. 5, pp. 839–842, May 2003.

[22] X. Vives, "Complementarities and games: New developments," *Journal of Economic Literature*, vol. 43, no. 2, pp. 437–479, June 2005.

[23] P. Milgrom and J. Roberts, "Rationalizability, learning, and equilibrium in games with strategic complementarities," *Econometrica*, vol. 58, no. 6, pp. 1255–77, Nov. 1990.

[24] D. Tse and P. Viswanath, *Fundamentals of Wireless Communication*. New York, NY, USA: Cambridge University Press, 2005.

[25] N. Nisan, T. Roughgarden, E. Tardos, and V. V. Vazirani, *Algorithmic Game Theory*. New York, NY, USA: Cambridge University Press, 2007.

[26] C. Papadimitriou, "Algorithms, games, and the internet," in *STOC '01: Proceedings of the thirty-third annual ACM symposium on Theory of computing*. New York, NY, USA: ACM, 2001, pp. 749–753.

[27] A. Lozano, A. Tulino, and S. Verdu, "High-SNR power offset in multiantenna communication," *Information Theory, IEEE Transactions on*, vol. 51, no. 12, pp. 4134–4151, Dec. 2005.

[28] E. Larsson and E. Jorswieck, "Competition versus cooperation on the MISO interference channel," *Selected Areas in Communications, IEEE Journal on*, vol. 26, no. 7, pp. 1059–1069, Sept. 2008.

Digital Object Identifier: 10.4108/ICST.VALUETOOLS2009.7793
http://dx.doi.org/10.4108/ICST.VALUETOOLS2009.7793